The Journal of Chemical Physics

Importance of van der Waals effects on the hydration of metal ions from the Hofmeister series

Cite as: J. Chem. Phys. **150**, 124505 (2019); https://doi.org/10.1063/1.5086939
Submitted: 25 December 2018 . Accepted: 04 March 2019 . Published Online: 27 March 2019

Liying Zhou, Jianhang Xu, Limei Xu, and Xifan Wu

The Journal of Chemical Physics ARTICLE scitation.org/journal/jcp

Importance of van der Waals effects on the hydration of metal ions from the Hofmeister series

Cite as: J. Chem. Phys. 150, 124505 (2019); doi: 10.1063/1.5086939
Submitted: 25 December 2018 • Accepted: 4 March 2019 •
Published Online: 27 March 2019

Liying Zhou,[1] Jianhang Xu,[2] Limei Xu,[1,3,a)] and Xifan Wu[2,a)]

AFFILIATIONS

[1]International Center for Quantum Materials, School of Physics, Peking University, Beijing 100871, People's Republic of China
[2]Department of Physics, Temple University, Philadelphia, Pennsylvania 19122, USA
[3]Collaborative Innovation Center of Quantum Matter, Beijing 100871, People's Republic of China

[a)]**Authors to whom correspondence should be addressed:** limei.xu@pku.edu.cn and xifanwu@temple.edu

ABSTRACT

The van der Waals (vdW) interaction plays a crucial role in the description of liquid water. Based on *ab initio* molecular dynamics simulations, including the non-local and fully self-consistent density-dependent implementation of the Tkatchenko-Scheffler dispersion correction, we systematically studied the aqueous solutions of metal ions (K^+, Na^+, and Ca^{2+}) from the Hofmeister series. Similar to liquid water, the vdW interactions strengthen the attractions among water molecules in the long-range, leading to the hydrogen bond networks softened in all the ion solutions. However, the degree that the hydration structure is revised by the vdW interactions is distinct for different ions, depending on the strength of short-range interactions between the hydrated ion and surrounding water molecules. Such revisions by the vdW interactions are important for the understanding of biological functionalities of ion channels.

I. INTRODUCTION

The nature of the interactions between hydrated ions from the Hofmeister series[1] and their surrounding water molecules plays a key role in understanding several fundamental physiological phenomena. For example, during the process of signal transduction, the selective permeability of the ligand-gated ion channels that allows the K^+, Na^+, or Ca^{2+} to pass through membranes is crucially dependent on the subtle details in their solvation structures.[2–4] Therefore, uncovering the precise picture of ion hydration continues to be at the center of scientific interest.[5–10] During the past years, state-of-the-art scattering and spectroscopy techniques have been developed and employed in experiments.[11–13] Complementary to the experimental approaches, *ab initio* molecular dynamics (AIMD) simulation[14,15] provides an ideal theoretical framework to study ion hydration in aqueous solution. Within the AIMD simulations, the hydrogen-bond (H-bond) network, under thermal fluctuation, and its dynamical interaction with hydrated ions are both modeled at a finite temperature. For the electronic degrees of freedom, a direct quantum mechanical treatment is allowed since the forces are computed from the ground state determined by density functional theory (DFT).[16] Therefore, AIMD simulations can describe the solvated ions at the molecular level, with the spatial and temporal resolutions that are inaccessible by current experiments.

Despite extensive AIMD simulations in aqueous solutions for over two decades, uncertainty remains. The accuracy of the predicted H-bond network critically depends on the level of exchange correlation approximations for the interacting electrons. To date, most AIMD simulations adopted the semilocal approximations at the generalized-gradient approximation (GGA) level, such as Perdew-Burke-Ernzerhof (PBE)[17] and Becke-Lee-Yang-Parr (BLYP)[18,19] functionals. Although the computed liquid structures are in qualitative agreement with experiments, it is widely recognized that GGA functionals predicted an over tetrahedrally structured water compared to available scattering experiments.[20] The overestimated H-bond strength originates partially from the self-interaction error[21] inherited from the semilocal approximation, artificially facilitating the donation of proton to oxygen lone pair electrons.[22] Furthermore, even more severe drawbacks arise from the neglect of the non-local exchange correlation effects

that are responsible for long-range van der Waals (vdW) interactions/dispersion forces.[23] It has been repeatedly shown that considering vdW interactions in GGA-AIMD simulations not only softens the H-bond structure towards the experimental direction but also is the key physical effect underlying the greater density of water than that of ice.[24–29]

Embedded in the H-bond network,[30] the first solvation shell of hydrated ions can be described by a polyhedron with each vertex occupied by a water molecule. In general, more than one type of polyhedron can be identified, indicating the competing nature among different solvation patterns under thermal fluctuation. The softened liquid structure by the vdW interactions can tilt the delicate balance with the free energy profiles, thus introducing non-trivial revisions to the ion hydration. Recently, it was found that the vdW interactions introduce major revisions to the hydration of water ions which revised the traditional mechanism of proton transfer.[31] Due to the emerging importance, whether vdW interactions have universal or rather ion-specific effects on the solvated Hofmeister cations, especially for the solvation structures which are important for the understanding of biological functionalities of ion channels, has not been well addressed.

To address the above issues, here we perform a systematic study of K^+, Na^+, and Ca^{2+} hydrations in aqueous solutions by considering the long-range vdW interactions based on PBE-AIMD simulations. In particular, we adopt the recently developed non-local and fully self-consistent implementation of Tkatchenko and Scheffler vdW (TS-vdW) correction.[22,32,33] Since the dispersion coefficients are computed as an explicit functional of the charge density, TS-vdW can capture the local chemical environment on-the-fly. Under the influence of vdW interactions, the increased interstitial water population softens the ion solvation structures within a less polarizable solvent. Accordingly, the hydration structures represented by the polyhedra with larger number of vertices are more stabilized. However, the extent to which the ion hydration is revised under the influence of dispersion forces differs significantly for different three metal ions, relying on the nature (size and charge) of the hydrated ion which decides the short-range interactions between the ion and surrounding water molecules. Namely, the rather flexible hydrations of K^+ undergo the largest revisions while the hydrations of Na^+ only gently perturbed. For the case of Ca^{2+}, the rather rigid solvation shells barely changed by the vdW interactions. Interestingly, the ordering of the ability of ions solvating water molecules and forming hydration structures is in accordance with the ionic ordering in the Hofmeister series, and such a phenomenon becomes more obvious when the vdW interactions are taken into account.

II. SIMULATION DETAILS

Born-Oppenheimer molecular dynamics have been performed based on DFT within the canonical ensemble as implemented in a modified version of the Quantum ESPRESSO[34,35] code package. Each of the three aqueous solutions studied here (K^+, Na^+, and Ca^{2+} aqueous solutions) was modeled by a periodic cubic cell with the size of 12.44 Å and a target temperature of 363 K, consisting of one ion and 63 water molecules. Simulations for pure water were also carried out with 64 water molecules using identical size as a benchmark. We adopted the PBE exchange correlation approximation combining with a fully self-consistent implementation of the density-dependent dispersion correction of TS-vdW

$$E_{\text{TS-vdW}}[\rho(\mathbf{r})] = -\frac{1}{2}\sum_{AB}\frac{f_{AB}[\rho(\mathbf{r})]C_{6,AB}[\rho(\mathbf{r})]}{R_{AB}^6}. \quad (1)$$

See Ref. 22 for more detailed information about Eq. (1). The interactions between valence electrons and the ion (comprising the nuclei and their corresponding frozen-core electrons) were approximated by the pseudopotential approach, in which the Hamann-Schlüter-Chiang-Vanderbilt[36,37] construction was used for H($1s^1$), O($2s^2 2p^4$), and K($3s^2 3p^6 4s^1$), SG15 optimized norm conserving Vanderbilt[38–40] was used for Ca($3s^2 3p^6 4s^2$), and Goedecker-Teter-Hutter[41] was used for Na($2s^2 2p^6 3s^1$). A cutoff energy of 85 Ry was used in the plane-wave expansions, and the Brillouin zone was sampled at the Γ point. All the AIMD trajectories have been equilibrated by over 30 ps, in which the Nose-Hoover thermostats[42] are applied to control the target temperature at 363 K. The hydrogen atoms were replaced with deuterium in order to maximize the allowable time step in the integration of the equations of motion and reduce the importance of quantum nuclear effects.[43,53] Such replacement did not affect the structural properties in the simulations in which the ions were treated as classical particles. In K^+ and Ca^{2+} AIMD trajectories, a time step of 0.48 fs was used for the molecular dynamics. For the case of Na^+, a time step of 0.36 fs was used. At each molecular dynamics time step in all AIMD trajectories, the wavefunction was fully relaxed and the electronic ground state was considered to be achieved if the difference in the total energy was equal or less than 0.5×10^{-7} Hartree between two consecutive steps of damped dynamics[44] on electrons.

III. RESULTS AND DISCUSSION

It is well known that the semilocal functional significantly overestimates the strength of H-bond, resulting in a sluggish liquid that barely diffuses at room temperature.[22] In order to mimic water under ambient conditions, much higher temperatures are commonly applied.[45–47] Even under the elevated temperature at 363 K in current simulations, the resulting over-structured H-bond network can be clearly seen in the oxygen-oxygen radial distribution function $g_{oo}(r)$ of the solvent water as shown in Figs. 1(a)–1(c). For all the three aqueous solutions, the first maximum and minimum of $g_{oo}(r)$ are predicted to be $g_{oo}^{max1}(r) = 2.92–3.00$ at $r^{max1} = 2.70–2.73$ Å and $g_{oo}^{min1}(r) = 0.49–0.59$ at $r^{min1} = 3.29–3.32$ Å, respectively (see Table I for detailed values). The previous results of combined X-ray and neutron diffraction data in pure liquid water[48] are also given in the last row of Table I for comparison. A higher first peak as well as a deeper first minimum in the $g_{oo}(r)$ is consistent with the fact that liquid water by PBE-AIMD is over-structured. When the vdW interactions are taken into account in the PBE+TS-vdW AIMD trajectories, the above drawback is largely improved. Unlike the vector nature of the H-bond pointing from the proton to the oxygen lone electron pair, the vdW interactions apply non-directional attractive forces to all the water molecules in the long-range. The strengthened attractions among water molecules soften the coordination shell of water solvent, evidenced by the systematically decreased average number of H-bonds (utilizing the definition proposed by Luzar and Chandler[49]) from 3.65-3.72 in PBE-AIMD to 3.54-3.56 in PBE+TS-vdW-AIMD trajectories similarly in the solvent of all three ion solutions in Figs. 1(d)–1(f) (see Table I for detailed values). As

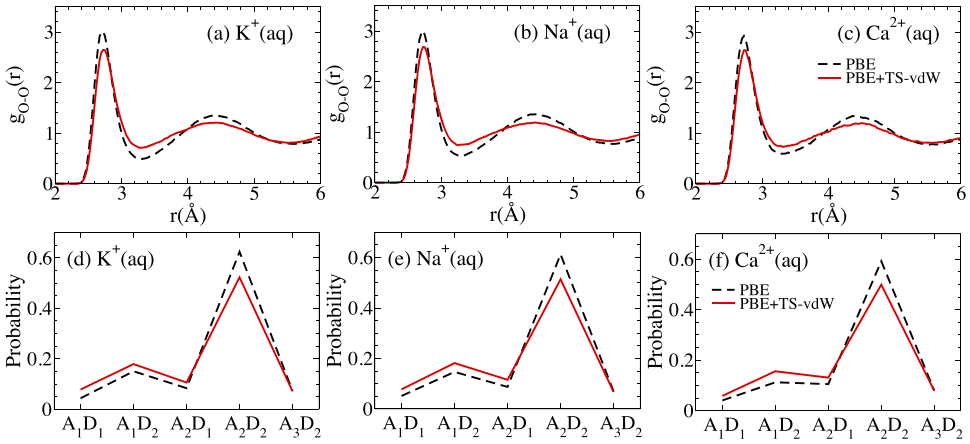

FIG. 1. The O–O radial distribution functions $g_{oo}(r)$ for K^+ (a), Na^+ (b), and Ca^{2+} (c) aqueous solution (aq) at the PBE and PBE+TS-vdW levels. The probability distributions for different types of H-bonds in K^+(d), Na^+ (e), and Ca^{2+} (f) aqueous solution at the PBE and PBE+TS-vdW levels. The x-axis label AxDy represents the number of accepted (Ax) and the number of donated (Dy) H-bonds, respectively. All other types of H-bonds have contributions less than 8% and are neglected for clarity.

a result, the non-bonded water molecules perturbed by vdW interactions enter the region between the first and second coordination shell and increase the population of interstitial water as shown by the less deep first minimum in Figs. 1(a)–1(c). In all the aqueous solutions under consideration, the correction by the vdW interactions on the oxygen-oxygen radial distribution function $g_{oo}(r)$ is rather similar, yielding $g_{oo}^{max1}(r)$ = 2.64–2.68 at r^{max1} = 2.73–2.74 Å and $g_{oo}^{min1}(r)$ = 0.71–0.74 at r^{min1} = 3.25–3.31 Å towards the experimental direction, respectively (see Table I for detailed values). It is also noted that the vdW effects on the $g_{oo}(r)$ is similar to the recent studies on pure liquid water using a similar approach.[22]

Under the influence of long-range vdW interactions, the ion hydration structures undergo additional attraction in a similar way as described in the H-bond network in water. As a result, the water molecules in the first and second coordination shells of solvated ions are brought closer in all the three ion solutions, facilitated by the attractive dispersion forces that are non-directional in nature. However, to what extent the hydration structure is revised by vdW interactions is distinct for each individual ion, as shown in Figs. 2(a)–2(i) and Table II.

Among all the three ions, the monovalent charged potassium ion has the largest ion size with the ion radius of 1.38 Å. Not surprisingly, the solvated K^+ also exhibits the most flexible hydration structure, which can be identified by the potassium-oxygen pair distribution function $g_{KO}(r)$ as shown in Fig. 2(a). Comparing the three ion solutions, the $g_{KO}(r)$ has the least structured first coordination shell with the first maximum located at r^{max1} = 2.70 Å, in good agreement with the experimental value of 2.73 Å determined by extended X-ray absorption fine-structure spectroscopy (EXAFS),[50] followed by a rather weak second coordination shell whose maximum position is at r^{max2} = 4.60 Å at the PBE level. Noticeably, the relatively less shallow first minimum, located at r^{min1} = 3.55 Å, indicates an increase in the population of water molecules in the interstitial region, with the coordination number (CN) of 6.00. The structural characteristic between the solvated K^+ and the molecules in its first hydration shell can be conveniently depicted by the polyhedra with each vertex hosting one water molecule. The rather flexible hydration structure of K^+ makes such polyhedra compatible with a broad spectrum in terms of vertex count, spanning from 4 to 10 as shown in Fig. 2(d), in comparison with 6 ± 2 detected by EXAFS.[50]

TABLE I. Tabulated summary of the structural properties of aqueous solutions obtained via the AIMD simulations performed in this work. From left to right, the positions (in Å) and intensities of the first maximum (r^{max1} and $g_{oo}^{max1}(r)$), the first minimum (r^{min1} and $g_{oo}^{min1}(r)$) of the corresponding oxygen-oxygen radial distribution function $g_{oo}(r)$; the average number of H-bonds (n_{HB}) per water molecule. The available experimental data are provided in the last row.

System	Method	r^{max1}	$g_{oo}^{max1}(r)$	r^{min1}	$g_{oo}^{min1}(r)$	n_{HB}
K^+	PBE	2.70	3.00	3.29	0.49	3.72
	PBE+TS-vdW	2.73	2.65	3.29	0.71	3.56
Na^+	PBE	2.73	3.00	3.32	0.53	3.68
	PBE+TS-vdW	2.73	2.68	3.25	0.74	3.54
Ca^{2+}	PBE	2.73	2.92	3.31	0.59	3.65
	PBE+TS-vdW	2.74	2.64	3.31	0.73	3.54
Pure water	Expt.[48]	2.76	2.62	3.42	0.82	...

TABLE II. Tabulated summary of the structural properties of aqueous solutions obtained via the AIMD simulations performed in this work. From left to right, the positions (in Å) and intensities of the first maximum (r^{max1} and $g_{ion\text{-}o}^{max1}(r)$), the first minimum ($r^{min1}$ and $g_{ion\text{-}o}^{min1}(r)$), and the second maximum (r^{max2} and $g_{ion\text{-}o}^{max2}(r)$) of the corresponding ion-oxygen radial distribution function $g_{ion-o}(r)$; the coordination number (CN) of the three ions; and the average dipole moment μ (in Debye) per water molecule belonging to the first solvation shell of the three ions. The available experimental peak position are provided for comparison.

Solution	Method	r^{max1}	$g_{ion\text{-}o}^{max1}(r)$	r^{min1}	$g_{ion\text{-}o}^{min1}(r)$	r^{max2}	$g_{ion\text{-}o}^{max2}(r)$	CN	μ
K^+	PBE	2.70	3.40	3.55	0.61	4.60	1.32	6.00	2.99
	PBE+TS-vdW	2.80	3.18	3.70	0.74	4.71	1.08	7.66	2.93
	Expt.[50]	2.73	...	...	...	...	...	...	...
	Expt.[52]	2.81	...	...	...	...	...	...	...
Na^+	PBE	2.38	5.13	3.23	0.22	4.42	1.43	5.12	3.00
	PBE+TS-vdW	2.41	4.62	3.23	0.41	4.37	1.25	5.15	2.95
	Expt.[12]	2.37	...	...	...	...	...	...	...
	Expt.[12]	2.38	...	...	...	...	...	...	...
Ca^{2+}	PBE	2.37	9.59	3.16	0.00	4.42	2.07	6.00	3.33
	PBE+TS-vdW	2.38	9.63	3.04	0.002	4.39	2.09	6.00	3.36
	Expt.[13]	2.38	...	...	...	...	...	...	...
	Expt.[58]	2.39	...	...	...	...	...	...	...

Within the PBE functional approximation, these polyhedra describing the first hydration shell of K^+ are dominated by square pyramid (CN = 5), pentagonal pyramids and octahedrons (CN = 6), and pentagonal bipyramids and triangular prisms (CN = 7) as shown in Fig. 2(d). Consistently, there are two noticeable peaks in the O–K–O angle distribution function as shown in Fig. 2(g). The main peak around 90° originates from the fact that the line connecting the apical oxygens and the K^+ is approximately normal to the base plane in polyhedra with CN = 5 and 6. The satellite peak around 55° is intrinsically from the polyhedra with a relatively larger number of vertices (CN ≥ 7). At the PBE+TS-vdW level, the vdW interactions apply long-range forces attracting the water molecules between the first and second coordination shells. Due to the flexible hydration shell, the above attraction can be seen by an obvious outward

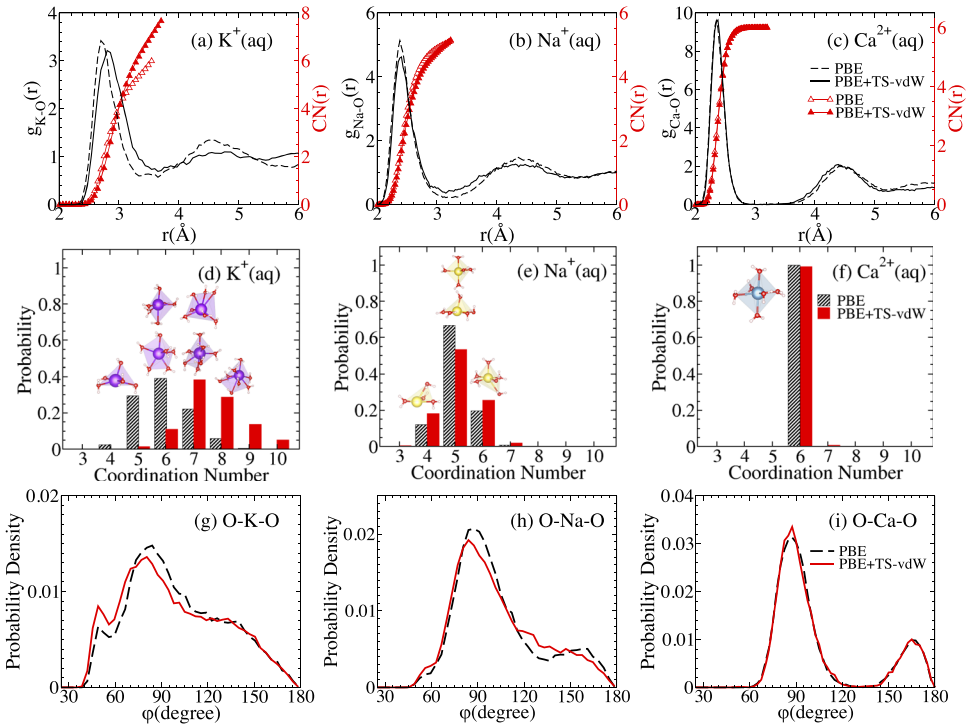

FIG. 2. The ION–O radial distribution functions (a) $g_{K-O}(r)$, (b) $g_{Na-O}(r)$, and (c) $g_{Ca-O}(r)$ at the PBE and PBE+TS-vdW levels. The red hollow triangles and red solid triangles in each panel represent the corresponding running coordination number CN(r) at the PBE and PBE+TS-vdW levels, respectively. With the x-axis ending at the first minimum r^{min1} of the ION–O radial distribution functions, the terminal points of CN(r) give the evaluated CN for the three ions at the PBE and PBE+TS-vdW levels. The probability distributions of CN for K^+ (d), Na^+ (e), and Ca^{2+} (f) at the PBE and PBE+TS-vdW levels. The typical hydration structures for K^+, Na^+, and Ca^{2+} with different CNs are presented. Red, white, purple, yellow, and cyan balls refer to O, H, K, Na, and Ca atoms, respectively. The angle distribution functions of O–ION–O φ for water molecules in the first solvation shell of K^+ (g), Na^+ (h), and Ca^{2+} (i) at the PBE and PBE+TS-vdW levels.

movement of the first coordination shell (r^{max1} = 2.80 Å and r^{min1} = 3.70 Å) in Fig. 2(a), consistent with previous simulation results,[51] and the X-ray and neutron diffraction experiments for KCl aqueous solutions with a K–O distance of 2.81 Å.[52] At the same time, the second coordination shell is destructed with a largely smeared peak due to the rather flexible hydration shell, allowing more water molecules to populate in the interstitial region. As a result, such a significant expansion of hydration volume by the dispersion forces enables K^+ to solvate more water molecules within its first coordination shell as shown in Fig. 2(a), which weakens the K^+-water interaction, with an increased CN of 7.66. Therefore, the first hydration shell is dominated by polyhedra with larger number of vertices [Fig. 2(d)]. In turn, it shifts the position of the main peak in the O–K–O angle distribution function to be further smaller than 90° and increases the magnitude of the peak around 55° [Fig. 2(g)] because of the increased population of polyhedra corresponding to CN = 7 influenced by the vdW interactions [Fig. 2(d)]. Such a tendency has also been observed from previous simulation results.[53]

The sodium ion carries a single positive charge as well. However, it has a smaller ion radius of 1.02 Å compared to that of K^+ due to its more compact electronic configuration of $1s^2 2s^2 2p^6$. Consequently, the interaction between Na^+ and its surrounding water molecules is stronger, which can be seen from the closer and more structured coordination shells in Fig. 2(b) compared to those in K^+ solution. At the PBE level, the first maximum r^{max1}, the first minimum r^{min1}, and the second maximum r^{max2} of the pair distribution function g_{Na-O} are located at 2.38 Å, 3.23 Å, and 4.42 Å, respectively. The location of the first maximum is in good agreement with the recent X-ray diffraction (XRD) and EXAFS experimental values of 2.38 Å and 2.37 Å, respectively.[12] Consistent with its more rigid hydration structure, the solvation complexes are dominated by the polyhedra with five vertices (CN = 5), represented by both the square pyramid and triangular bipyramid in Fig. 2(e), which has been reported in previous theoretical studies.[54] Such more rigid hydration structures give rise to the main peak of the O–Na–O angle distribution function centered at 90° followed by a second broader peak at around 170° [Fig. 2(h)]. In addition, tetrahedron (CN = 4) and octahedron (CN = 6) complexes are also found but with small fractions at the PBE level, suggesting a higher free energy than that of the solvation complex with CN = 5. At the PBE+TS-vdW level, the attraction among water molecules in the long-range distance is strengthened as usual. However, unlike the vdW effects in K^+ solution that significantly weakens the ion-water interaction, the first hydration shell of Na^+ is only gently perturbed with r^{max2} = 2.41 Å and becomes less structured. This difference is due to the stronger Na^+-water interaction than the K^+-water interaction. More obvious vdW effects can be observed from the second coordination shell, which is not only less structured but also closer to the first shell with r^{max2} = 4.37 Å [Fig. 2(b)]. The less structured hydration shells in turn make more water molecules populate in the interstitial region, resulting in a lifted first minimum in Fig. 2(b). Consistently, the majority of solvation complexes are still comprised by polyhedra with five vertices, but are more broadly distributed with a preference towards a larger number of vertices as shown in Fig. 2(e), with the CN increasing to 5.15 from 5.12. These values are consistent with the experimental data of 5.2 and 5.5 determined by X-ray absorption spectroscopy (XAS)[11] and XRD,[12] respectively. Under the influence of increased interstitial water fluctuations, most of the solvation complexes are perturbed and more distorted polyhedra are identified. As a result, the main peak of the O–Na–O angle distribution function shifts from 90° to an acute angle at 84°, and the second broad peak decreases slightly too, as shown in Fig. 2(h). Similar effects have been recently reported in pure liquid water[22] as well as solvated water ions in aqueous solutions.[51,53]

The calcium ion bears two positive charges with the smallest ion radius of 0.99 Å among the three ions. Solvated in water, it presents the strongest ion-water interaction via its high electrostatic field among the three ion solutions, indicated by the pair distribution function g_{Ca-O} in Fig. 2(c), showing that the first hydration shell is much more closer to the Ca^{2+} than K^+ and Na^+. At the PBE level, the first maximum r^{max1}, the first minimum r^{min1}, and the second maximum r^{max2} are located at 2.37 Å, 3.16 Å, and 4.42 Å, respectively. Meanwhile, both the first and second coordination shells are much more structured than those of K^+ and Na^+, and the octahedron with CN = 6 [Fig. 2(f)] is found to be the only stable solvation complex at the PBE level, consistent with previous studies.[55–57] It turns out that the octahedron solvation complexes are responsible for the two sharp peaks at 90° and 165° in the O–Ca–O angle distribution function in Fig. 2(i). The rather rigid hydration shell of solvated Ca^{2+} induces a unique effect under the influence of vdW interactions, i.e., the first hydration shell is nearly intact (r^{max1} = 2.38 Å), consistent with the recent experimental data of 2.38 Å determined by neutron scattering,[13] and the entire second hydration shell only slightly moves inwards (from 4.42 Å to 4.39 Å) with its shape almost unchanged perturbed by the attractive vdW forces. At the PBE+TS-vdW level, the octahedron with CN = 6 is also the most stable solvation complex with only a negligible increased fraction of complex with CN = 7. As expected, the O–Ca–O angle distribution function barely changes when considering the vdW interactions as shown in Fig. 2(i).

The electric properties of the water molecules in ion solutions also undergo non-trivial changes due to the vdW effects. The electric dipole moment of water molecules in the liquid condensed phase (2.9*D*)[59] is much higher than that of the gas phase (1.85*D*),[60,61] which is attributed to the poling effect via the H-bonding. At the PBE level, the artificially strengthened H-bonding yields an overestimated electric dipole moment μ_w = 3.16*D* in pure liquid water, computed from the maximally localized Wannier functions (MLWF)[62,63]

$$\mu = R_{H_1} + R_{H_2} + 6R_O - 2\sum_{i=1}^{4} R_{W_i}, \tag{2}$$

in which R_{H_1}, R_{H_2}, and R_O are the Cartesian coordinates of the hydrogen and oxygen atoms comprising the water molecule, respectively, and R_{W_i} are the coordinates of the four corresponding MLWF centers. As a measurement of the ability of the hydrated ion to polarize surrounding water molecules, the electric dipole moment of the water molecules in the first coordination shell of hydrated ions are predicted to be 2.99*D* (0.95 × μ_w), 3.00*D* (0.95 × μ_w), and 3.33*D* (1.05 × μ_w) in K^+, Na^+, and Ca^{2+} solutions, respectively. The above is consistent with the assignment of Ca^{2+} as the *structure-maker*, K^+ as the *structure-breaker*, and Na^+ as the weak *structure-breaker*.[10,29] After the long-range vdW interactions are taken into account, the softened liquid water structure becomes less polarizable, with the average electric dipole moment per water molecule in pure liquid water μ_{w-v} = 3.05*D*, close to the experimental value

of 2.9D, which has been reported in a previous theoretical study,[22] and the electric dipole moment of the water molecules in the first coordination shell of hydrated ions are predicted to be 2.93D (0.96 × μ_{w-v}), 2.95D (0.97 × μ_{w-v}), and 3.36D (1.10 × μ_{w-v}) in K^+, Na^+, and Ca^{2+} solutions, respectively. In fact, the increase in CN for K^+ and Na^+ originating from the dispersion forces weakens the interactions between the hydrated ion and water molecules in the first coordination shell, leading to the polarization of neighboring water molecules becoming closer to that of in pure liquid water at the PBE+TS-vdW level. However, for the case of Ca^{2+}, the interactions between the ion and neighboring water molecules are so strong that they are less affected by the long-range vdW attraction originating from the coupled dipole fluctuations non-locally;[23] therefore, the interactions between Ca^{2+} and water molecules in its first hydration shell are relatively enhanced, resulting in more polarized surrounding water molecules. Interestingly, the hydrated Ca^{2+} becomes an even stronger *structure-maker*, while the role played by K^+ ~ Na^+ as the *structure-breaker* is even slightly weaker, which is in agreement with the experimental estimation.[64]

IV. CONCLUSIONS

We have performed a systematic study on the hydration of metal ions (K^+, Na^+, and Ca^{2+}) from the Hofmeister series, based on a semilocal density functional approximation including the nonlocal and fully self-consistent density-dependent implementation of the Tkatchenko-Scheffler dispersion correction within the framework of AIMD simulations. Similar to liquid water, the H-bond networks in all the ion solutions are found to be softened under the influence of vdW interactions, strengthening the attractions among water molecules in the long-range. However, the vdW interactions have ion-specific effects on the solvated Hofmeister cations considered here, relying on the nature (size and charge) of the hydrated ion which decides the short-range interactions between the ion and surrounding water molecules. Thus, the rather flexible hydrations of K^+ undergo the largest revisions, and the solvation structures are dominated by polyhedra with larger number of vertices, while the hydrations of Na^+ only gently perturbed, with the majority of solvation complexes are still with five vertices but are more broadly distributed with a preference towards a larger number of vertices. For the case of Ca^{2+}, the rather rigid hydration shells barely changed by the vdW interactions, and the only stable solvation structure of octahedron is still the most stable solvation complex with only a negligible increased fraction of complex with CN = 7. The present results are consistent with the available experimental data. At the same time, we have computed the electric dipole moment of the water molecules in the first coordination shell of the hydrated ions using the methods of MLWF, and the results seem to consistent with the assignment of Ca^{2+} as the *structure-maker*, K^+ as the *structure-breaker*, and Na^+ as the weak *structure-breaker*[10] even though considering the vdW interactions. Our study shows that vdW interactions have vital effects on the hydration of metal ions from the Hofmeister series, in particular, on the subtle details of the solvation structures, which are the features with the biological functionalities such as the ion channels. Furthermore, the ordering of the ability of ions solvating water molecules and forming hydration structures is in accordance with the ionic ordering in the Hofmeister series, and such a phenomenon becomes more obvious when the vdW interactions are taken into account. Such observations suggest that a proper treatment of vdW interactions may be significant for the investigation of permeability through biological channels.

ACKNOWLEDGMENTS

L.Z. and L.X. acknowledge the National Basic Research Program of China (973 Program, Grant No. 2015CB856801), the National Natural Science Foundation of China (Grant No. 1152552), and the National Key Research and Development Program of China (Grant No. 2016YFA0300901). We were grateful for the computational resources provided by the TianHe-1A and the High-performance Computing Platform of Peking University. This work was supported by the Computational Chemical Center: Chemistry in Solution and at Interfaces funded by the DoE under Award No. DE-SC0019394 (to X.W.). This research used resources of the National Energy Research Scientific Computing Center (NERSC), a DOE Office of Science User Facility supported by Office of Science of the U.S. DOE Contract No. DE-AC02-05CH11231.

REFERENCES

[1] F. Hofmeister, Arch. Exp. Pathol. Pharmacol. **25**, 1–30 (1888).
[2] Y. Zhou, J. H. Morais-Cabral, A. Kaufman, and R. MacKinnon, Nature **414**, 43 (2001).
[3] L. G. Palmer, J. Membr. Biol. **67**, 91–98 (1982).
[4] E. Pidcock and G. R. Moore, J. Biol. Inorg. Chem. **6**, 479–489 (2001).
[5] P. R. Smirnov and V. N. Trostin, Russ. J. Gen. Chem. **77**, 2101–2107 (2007).
[6] P. R. Smirnov and V. N. Trostin, Russ. J. Gen. Chem. **77**, 844–850 (2007).
[7] P. R. Smirnov and V. N. Trostin, Russ. J. Gen. Chem. **79**, 1600–1607 (2009).
[8] C. W. Swartz and X. Wu, Phys. Rev. Lett. **111**, 087801 (2013).
[9] A. Bankura, B. Santra, R. A. DiStasio, Jr., C. W. Swartz, M. Klein, and X. Wu, Mol. Phys. **113**, 2842–2854 (2015).
[10] Y. Marcus, Chem. Rev. **109**, 1346–1370 (2009).
[11] H. J. Kulik, N. Marzari, A. A. Correa, D. Prendergast, E. Schwegler, and G. J. Galli, Phys. Chem. B **114**, 9594–9601 (2010).
[12] M. Galib, M. D. Baer, L. B. Skinner, C. J. Mundy, T. Huthwelker, G. K. Schenter, C. J. Benmore, N. Govind, and J. L. Fulton, J. Chem. Phys. **146**, 084504 (2017).
[13] T. Martinek, E. Duboué-Dijon, Š. Timr, P. E. Mason, K. Baxová, H. E. Fischer, B. Schmidt, E. Pluhařová, and P. J. Jungwirth, Chem. Phys. **148**, 222813 (2018).
[14] R. Car and M. Parrinello, Phys. Rev. Lett. **55**, 2471 (1985).
[15] D. Marx and J. Hutter, *Ab Initio Molecular Dynamics: Basic Theory and Advanced Methods* (Cambridge University Press, 2009).
[16] W. Kohn and L. J. Sham, Phys. Rev. **140**, A1133 (1965).
[17] J. P. Perdew, K. Burke, and M. Ernzerhof, Phys. Rev. Lett. **77**, 3865 (1996).
[18] A. D. Becke, Phys. Rev. A **38**, 3098 (1988).
[19] C. Lee, W. Yang, and R. G. Parr, Phys. Rev. B **37**, 785 (1988).
[20] M. J. Gillan, D. Alfè, and A. J. Michaelides, J. Chem. Phys. **144**, 130901 (2016).
[21] J. P. Perdew and A. Zunger, Phys. Rev. B **23**, 5048 (1981).
[22] R. A. DiStasio, Jr., B. Santra, Z. Li, X. Wu, and R. J. Car, Chem. Phys. **141**, 084502 (2014).
[23] J. Klimeš and A. Michaelides, J. Chem. Phys. **137**, 120901 (2012).
[24] J. Schmidt, J. VandeVondele, I. F. W. Kuo, D. Sebastiani, J. I. Siepmann, J. Hutter, and C. J. Mundy, J. Phys. Chem. B **113**, 11959–11964 (2009).
[25] J. Wang, G. Román-Pérez, J. M. Soler, E. Artacho, and M. V. Fernández-Serra, J. Chem. Phys. **134**, 024516 (2011).
[26] I. C. Lin, A. P. Seitsonen, I. Tavernelli, and U. J. Rothlisberger, Chem. Theory Comput. **8**, 3902–3910 (2012).
[27] A. Bankura, A. Karmakar, V. Carnevale, A. Chandra, and M. L. Klein, J. Phys. Chem. C **118**, 29401–29411 (2014).

[28]T. Ikeda and M. Boero, J. Chem. Phys. **143**, 194510 (2015).
[29]G. Miceli, S. de Gironcoli, and A. Pasquarello, J. Chem. Phys. **142**, 034501 (2015).
[30]M. Chen, H. Y. Ko, R. C. Remsing, M. F. C. Andrade, B. Santra, Z. Sun, A. Selloni, R. Car, M. L. Klein, J. P. Perdew, and X. Wu, Proc. Natl. Acad. Sci. U. S. A. **114**, 10846–10851 (2017).
[31]M. Chen, L. Zheng, B. Santra, H. Y. Ko, R. A. DiStasio, Jr., M. L. Klein, R. Car, and X. Wu, Nat. Chem. **10**, 413 (2018).
[32]A. Tkatchenko and M. Scheffler, Phys. Rev. Lett. **102**, 073005 (2009).
[33]N. Ferri, R. A. DiStasio, Jr., A. Ambrosetti, R. Car, and A. Tkatchenko, Phys. Rev. Lett. **114**, 176802 (2015).
[34]P. Giannozzi, S. Baroni, N. Bonini, M. Calandra, R. Car, C. Cavazzoni *et al.*, J. Phys.: Condens. Matter **21**, 395502 (2009).
[35]P. Giannozzi, O. Andreussi, T. Brumme, O. Bunau, M. B. Nardelli, M. Calandra *et al.*, J. Phys.: Condens. Matter **29**, 465901 (2017).
[36]D. R. Hamann, M. Schlüter, and C. Chiang, Phys. Rev. Lett. **43**, 1494 (1979).
[37]D. Vanderbilt, Phys. Rev. B **32**, 8412 (1985).
[38]D. R. Hamann, Phys. Rev. B **88**, 085117 (2013).
[39]M. Schlipf and F. Gygi, Comput. Phys. Commun. **196**, 36–44 (2015).
[40]P. Scherpelz, M. Govoni, I. Hamada, and G. Galli, J. Chem. Theory Comput. **12**, 3523 (2016).
[41]S. Goedecker, M. Teter, and J. Hutter, Phys. Rev. B **54**, 1703 (1996).
[42]G. J. Martyna, M. L. Klein, and M. Tuckerman, J. Chem. Phys. **97**, 2635 (1992).
[43]Z. Sun, Li. Zheng, M. Chen, M. L. Klein, F. Paesani, and X. Wu, Phys. Rev. Lett. **121**, 137401 (2018).
[44]F. Tassone, F. Mauri, and R. Car, Phys. Rev. B **50**, 10561 (1994).
[45]A. P. Gaiduk, C. Zhang, F. Gygi, and G. Galli, Chem. Phys. Lett. **604**, 89 (2014).
[46]J. C. Grossman, E. Schwegler, E. W. Draeger, F. Gygi, and G. Galli, J. Chem. Phys. **120**, 300 (2004).
[47]E. Schwegler, J. C. Grossman, F. Gygi, and G. Galli, J. Chem. Phys. **121**, 5400 (2004).
[48]A. K. Soper and C. J. Benmore, Phys. Rev. Lett. **101**, 065502 (2008).
[49]A. Luzar and D. Chandler, Phys. Rev. Lett. **76**, 928 (1996).
[50]V. A. Glezakou, Y. Chen, J. L. Fulton, G. K. Schenter, and L. X. Dang, Theor. Chem. Acc. **115**, 86 (2006).
[51]A. Bankura, V. Carnevale, and M. L. Klein, J. Chem. Phys. **138**, 014501 (2013).
[52]J. Mähler and I. Persson, Inorg. Chem. **51**, 425 (2011).
[53]A. Bankura, V. Carnevale, and M. L. Klein, Mol. Phys. **112**, 1448–1456 (2014).
[54]T. Ikeda, M. Boero, and K. Terakura, J. Chem. Phys. **126**, 034501 (2007).
[55]I. Bako, J. Hutter, and G. Palinkas, J. Chem. Phys. **117**, 9838 (2002).
[56]F. C. Lightstone, E. Schwegler, M. Allesch, F. Gygi, and G. Galli, ChemPhysChem **6**, 1745 (2005).
[57]T. Todorova, P. H. Hünenberger, and J. Hutter, J. Chem. Theory Comput. **4**, 779 (2008).
[58]M. M. Probst, T. Radnai, K. Heinzinger, P. Bopp, and B. M. Rode, J. Phys. Chem. **89**, 753 (1985).
[59]Y. S. Badyal, M. L. Saboungi, D. L. Price, S. D. Shastri, D. R. Haeffner, and A. K. Soper, J. Chem. Phys. **112**, 9206 (2000).
[60]S. A. Clough, Y. Beers, G. P. Klein, and L. S. Rothman, J. Chem. Phys. **59**, 2254 (1973).
[61]S. L. Shostak, W. L. Ebenstein, and J. S. Muenter, J. Chem. Phys. **94**, 5875 (1991).
[62]N. Marzari and D. Vanderbilt, Phys. Rev. B **56**, 12847 (1997).
[63]E. R. Batista, S. S. Xantheas, and H. Jónsson, J. Chem. Phys. **111**, 6011 (1999).
[64]K. A. Valiev and M. I. Emel'yanov, J. Struct. Chem. **5**, 625 (1965).